Polymer Chemistry

Accepted Manuscript

This is an *Accepted Manuscript*, which has been through the Royal Society of Chemistry peer review process and has been accepted for publication.

Accepted Manuscripts are published online shortly after acceptance, before technical editing, formatting and proof reading. Using this free service, authors can make their results available to the community, in citable form, before we publish the edited article. We will replace this *Accepted Manuscript* with the edited and formatted *Advance Article* as soon as it is available.

You can find more information about *Accepted Manuscripts* in the Information for Authors.

Please note that technical editing may introduce minor changes to the text and/or graphics, which may alter content. The journal's standard Terms & Conditions and the Ethical guidelines still apply. In no event shall the Royal Society of Chemistry be held responsible for any errors or omissions in this *Accepted Manuscript* or any consequences arising from the use of any information it contains.

ROYAL SOCIETY OF CHEMISTRY

www.rsc.org/polymers

Cite this: DOI: 10.1039/c0xx00000x

www.rsc.org/xxxxxx

ARTICLE TYPE

Galactosylated Reduction and pH Dual-Responsive Triblock Terpolymer Gal-PEEP-*a*-PCL-*ss*-PDMAEMA: a Multifunctional Carrier for Targeted and Simultaneous Delivery of Doxorubicin and DNA

Yang Zhang, Jinlin He*, Dongling Cao, Mingzu Zhang and Peihong Ni*

Received (in XXX, XXX) Xth XXXXXXXXX 20XX, Accepted Xth XXXXXXXXX 20XX
DOI: 10.1039/b000000x

For developing a multifunctional bioreducible system for targeted co-delivery of anticancer drug and DNA, novel galactosamine (Gal)-modified polymeric micelles with reduction (disulfide group, -*ss*-) and pH (acetal group, -*a*-) dual-responsive properties were constructed from poly(ethylethylene phosphate)-*a*-poly(ε-caprolactone)-*ss*-poly[2-(dimethylamino)ethyl methacrylate] (Gal-PEEP-*a*-PCL-*ss*-PDMAEMA) terpolymers. These multifunctional terpolymers were synthesized *via* a combination of ring-opening polymerization (ROP), atom transfer radical polymerization (ATRP) and Cu(I)-catalyzed azide-alkyne cycloaddtion (CuAAC) "click" reaction. The chemical structures and compositions, as well as the molecular weights and molecular weight distributions (PDIs) of these terpolymers have been fully characterized, and their self-assembly behavior were also studied in detail. The interaction between terpolymer and DNA was studied by agarose gel retardation assay, and the physical properties of resulting polyplexes were further determined by zeta potential, DLS, and TEM analyses. The micelles containing acetal and disulfide groups could be dissociated under intracellular environment. The reduction and pH-triggered release of doxorubicin (DOX) from DOX-loaded micelles showed that the release of DOX was obviously accelerated at pH 5.0 or pH 7.4 with 10 mM GSH, and the release rate was further enhanced at the condition of pH 5.0 with 10 mM GSH. MTT assay indicated that the blank micelles displayed relatively low cytotoxicity against HeLa cells and HepG2 cells. Although the DOX-loaded micelles could efficiently prohibit the growth of both cells, they exhibited much higher cytotoxicity against HepG2 cells than HeLa cells. In addition, the intracellular uptake and transfection of Gal-PEEP-*a*-PCL-*ss*-PDMAEMA /DNA/DOX polyplexes into HepG2 cells was more efficient than that of HeLa cells as revealed by a live cell imaging system owing to specific ligand-receptor interactions between Gal and asialoglycoprotein receptors (ASGPRs) overexpressed on the surface of HepG2 cells. The present study provides a facile strategy for the preparation of multifunctional biodegradable polymeric micelles that may act as a promising platform for targeted intracellular co-delivery of hydrophobic drugs and nucleic acids.

Introduction

Over the past decades, biocompatible and biodegradable amphiphilic copolymers have been considered the most prospective nanocarriers for the controlled delivery of drugs. They have displayed tremendous potentials to solve some critical issues encountered in traditional chemotherapy to a great extent, such as high toxicity to normal tissues, poor water solubility, sluggish drug release and no targeting effects.[1-3] Meanwhile, gene therapy using polymeric micelles as vactors has also been paid more attention because this stretagy would be a promising treatment method for various human diseases including cancers, genetic disorders, and viral infections.[4,5] Up to now, a great number of polyplexes of non-virus cationic polymer/DNA have been constructed to delivery genes into cells to achieve prolonged circulation, targeting delivery and enhanced gene trasfection.[6-9] However, it should be noted that most drug or gene delivery systems often suffer limited cellular uptake from the enhanced permeability and retention (EPR) effect and inefficient drug release at the tumor site, as well as low transfection in the cancer cells. These problems have brought new opportunities and challenges to the field of biomedical polymers.

In recent years, intracellular environment-sensitive polymeric nanocarriers that release drugs or genes in response to some specific signals, such as temperature, pH value, enzyme and cytoplasmic glutathione (GSH), have been widely applied in cancer therapy.[10-15] These self-assembled nanoparticles are relatively stable under physiological conditions, while their stimuli-triggered degradation in the tumor cells would result in a

Polymer Chemistry Accepted Manuscript

fast release of loaded cargos. For example, owing to the acidic environment in tumor tissues (*e.g.* pH 5.0-6.5 for endosomes, pH 4.5-5.0 for lysosomes, and 6.5-7.2 for extracellular tumor sites),[16,17] many researches focused on pH-sensitive polymeric micelles containing acid-cleavable groups including acetal,[18,19] hydrazone,[20,21], ortho ester[22,23], and oxime.[24,25] Very recently, we reported a triblock copolymer linked by acetal groups with rapid acid-triggered hydrolysis. The pH-responsive micelles based on biodegradable poly(ε-caprolactone)-*acetal*-poly(ethylene glycol)-*acetal*-poly(ε-caprolactone) (PCL-*a*-PEG-*a*-PCL) triblock copolymers could be dissociated when the acetal groups were cleaved under the intracellular environment and then resulted in a pH-triggered release of DOX.[26] Another appealing stimulus factor comes from redox potential in the cytosol and nuclei that contain 100 to 1000-fold higher concentration of reducing GSH tripeptide (*ca.* 1-10 mM) than common fluids outside cells (*ca.* 2-20 μM).[15,27-30] It was reported that tumor tissues are characterized with at least 4-fold higher GSH levels relative to normal tissues.[31] Therefore, in an effort to further improve the drug release performances, novel dual-responsive polymeric nanoparticles that can respond to a combination of pH and redox signals have recently been widely investigated because both of them exist naturally in certain pathological tissue as well as in all cancer cells.[32-36]

The concept of combination therapy in cancer was proposed and opened some possibilities for the delivery of multiple therapeutic agents.[37,38] If this techneque could be achieved, it would lead to significant benefits including a lower treatment failure, lower case-fatality ratios and slower development of multiple drugs resistance (MDR).[39-41] For example, aiming to combine the advantages of therapeutic anticancer drugs and nucleic acids, various multifunctional carriers have been constructed for the simultaneous delivery of both therapeutic agents,[42,43] including polymers,[44-47] liposomes,[48-50] dendrimers,[51,52] and inorganic nanoparticles (mesoporous SiO_2, Au, quantum dots, *etc.*).[53] Among them, hydrophobically-modified cationic polymers have attracted much attention because of some intrinsic advantages, such as good biocompatibility and biodegradability, easily-adjustable structures and functions. Most anticancer drugs and genes can be simultaneously encapsulated into these carriers *via* hydrophobic interaction and electrostatic interaction, respectively. More importantly, the surface of resulting complexes can be further modified with functional fluorescence or targeting ligands, which provides a new pathway to construct multifunctional vectors.[3]

Inspired by the aforementioned advantages, we herein report on a novel multifunctional nanoscaled terpolymeric system. It is composed of targeted galactosamine (Gal)-modified cationic terpolymers containing poly(ε-caprolactone) (PCL), poly(ethylethylene phosphate) (PEEP) and poly[2-(dimethylamino)ethyl methacrylate] (PDMAEMA) blocks, and linked by both reduction and pH dual-responsive bonds (abbreviated as Gal-PEEP-*a*-PCL-*ss*-PDMAEMA). This system is expected to have the following characteristics: (i) simultaneously encapsulating DNA and hydrophobic DOX, (ii) prolonging circulation time in blood by hydrophilic and biodegradable polyphosphoester shielding,[54-56] (iii) being recognized by asialoglycoprotein receptors (ASGPRs) overexpressing hepatoma cells and internalized *via* a receptor-mediated endocytosis process due to the introduction of Gal moieties.[38,57,58] As shown in Scheme 1, when the DOX and DNA-loaded polyplexes were internalized in target cells, the acetal bonds could be first cleaved under mildly acidic endosomal conditions and resulted in partial release of cargos; While once the polyplexes escaped from endosomes, cleavage of the disulfide linkages in response to a high concentration of GSH would lead to further complete release of DOX and DNA into the cytosol.

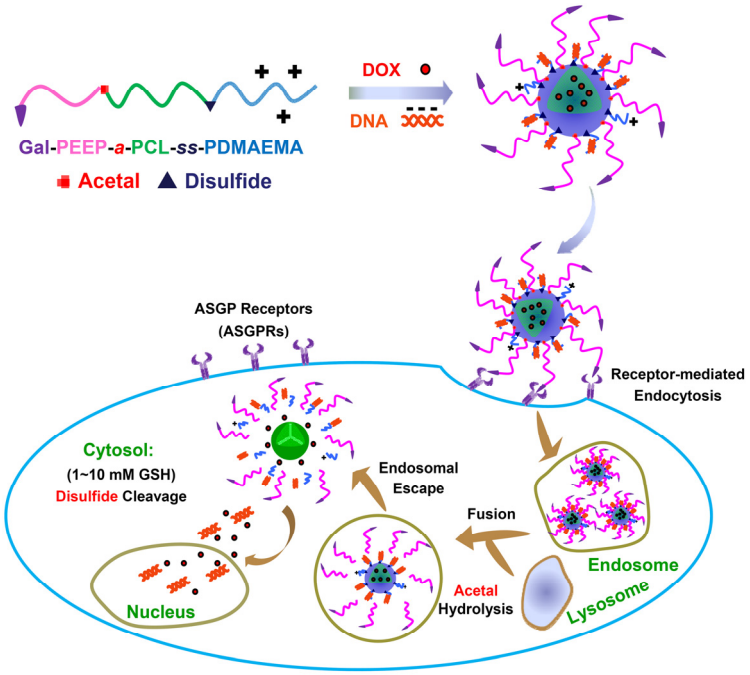

Scheme 1 Schematic illustration of reduction and pH dual-responsive triblock terpolymer Gal-PEEP-*a*-PCL-*ss*-PDMAEMA as the co-delivery carrier of DOX and DNA, as well as the triggered release of cargos under intracellular circumstance.

Polymer Chemistry Accepted Manuscript

This journal is © The Royal Society of Chemistry [year]

Experimental

Materials

2-Ethoxy-2-oxo-1, 3, 2-dioxaphospholane (EOP) was synthesized by a method described previously and distilled under vacuum just before use.[55] 2-(Dimethylamino)ethyl methacrylate (DMAEMA, 98%, Wuxi Xinyu Chemical Reagent) was dried over CaH_2 for 12 h and distilled under vacuum immediately before use. Stannous octoate [$Sn(Oct)_2$, 95%, Sigma-Aldrich] and triethylamine (TEA, Sinopharm Chemical Reagent) were also distilled under vacuum before use. 2, 2'-Bipyridine (bpy, 99%, Sinopharm Chemical Reagent), sodium azide (NaN_3, 98%, Sinopharm Chemical Reagent), pyridinium *p*-toluenesulfonate (PPTS, 98%, Acros), 2-chloroethyl vinyl ether (CEVE, 98%, TCI), *α*-bromoisobutyryl bromide (98%, Sigma-Aldrich), 2-hydroxyethyl disulfide (technical grade, Sigma-Aldrich), *N*, *N*, *N*', *N*", *N*"-Pentamethyl diethylenetriamine (PMDETA, 99%, J&K Chemical), calf thymus DNA (Sigma-Aldrich), pUC18 plasmid DNA (Takara), doxorubicin hydrochloride (DOX·HCl, 99%, Beijing Zhongshuo Pharmaceutical Technology Development), bisbenzimide Hoechst 33342 trihydrochloride (H 33342, 98%, Sigma-Aldrich), thiazolyl blue tetrazolium bromide (MTT, 98%, Sigma-Aldrich), D-(+)-galactosamine hydrochloride (98%, Shanghai Yuanju Biotechnology) and *N*, *N'*-carbonyldiimidazole (CDI, 98%, Shanghai Medpep) were used without further purification. Tetrahydrofuran (THF, A.R., Sinopharm Chemical Reagent) was initially dried over KOH for at least two days and then refluxed over sodium wire with benzophenone as indicator until the color turned to purple. ε-Caprolactone (ε-CL, 99%, Acros) was dried over CaH_2 for 24 h and distilled under vacuum before use. Cuprous bromide (CuBr, 95%, Sinopharm Chemical Reagent) was purified by washing with glacial acetic acid and acetone for three times, followed by drying under vacuum at 25 °C for 24 h. Toluene (A.R., Sinopharm Chemical Reagent) was dried through refluxing over CaH_2 and distilled before use. *N*, *N*-Dimethylformamide (DMF, A.R., Sinopharm Chemical Reagent) was dried over anhydrous $MgSO_4$ and distilled under vacuum before use. All the other reagents were obtained from Sinopharm Chemical Reagent and used as received.

Synthesis of homopolymer Cl-*a*-PCL-*ss*-Br

Synthesis of 2-[(2-hydroxyethyl)disulfanyl]ethyl 2-bromo-2-methylpropanoate (HO-ss-Br)

To a solution of 2-hydroxyethyl disulfide (10.0 g, 0.033 mol) and TEA (7.0 mL, 0.048 mol) dissolved in 100 mL of anhydrous THF, a mixture of *α*-bromoisobutyryl bromide (1.5 mL, 0.012 mol) with 10 mL of anhydrous THF was added dropwise at 0 °C over 30 min. The solution was then stirred at 25 °C for 12 h. The white precipitates formed during the reaction were removed by filtration and the filtrate was dried by rotary evaporation to remove THF. The remaining oil-like product was purified by flash column chromatography (silica gel) with a mixture of CH_2Cl_2/ethyl acetate (*v*/*v* = 5/1) as the eluent. The final product was isolated as a yellowish oil (4.39 g, yield: 34%, R_f = 0.68).

Synthesis of HO-PCL-ss-Br

To a 50 mL of dry flask containing 20 mL of anhydrous toluene was added with HO-*ss*-Br (0.189 g, 0.6 mmol), ε-CL (3.55 g, 0.03 mol) and $Sn(Oct)_2$ (0.126 g, 0.3 mmol). The flask was degassed through three exhausting-refilling dry nitrogen cycles, and the reaction was carried out at 90 °C for 4 h with continuous stirring. After that, the mixture was concentrated and precipitated twice in 150 mL of cold diethyl ether, the precipitates were then collected and dried under vacuum at 30 °C to a constant weight (3.15 g, yield: 84.3%).

Synthesis of Cl-a-PCL-ss-Br carrying disulfide and acetal groups

In order to remove the trace water in the reactants, HO-PCL-*ss*-Br (3.0 g, 0.45 mmol) and PPTS (22.5 mg, 0.09 mmol) were respectively dried by azeotropic distillation with anhydrous toluene just before use, and then dissolved in 30 mL of anhydrous CH_2Cl_2 in a 50 mL of dry flask. Under a dry nitrogen atmosphere, a solution containing 0.45 mL of CEVE (4.5 mmol) in 5 mL of anhydrous CH_2Cl_2 was added dropwise into the flask at 0 °C over 30 min. After further stirring for 30 min, the reaction was quenched by adding 10 mL of 5 wt% Na_2CO_3 aqueous solution. The mixture was diluted with 50 mL of CH_2Cl_2 and washed twice with 10 mL of PBS buffer solution (pH 10.0). The organic phase was dried over anhydrous $MgSO_4$ for 2 h, the filtrate was then concentrated and precipitated twice into 150 mL of cold hexanes. The precipitates were then collected and dried under vacuum at 30 °C to a constant weight to give Cl-*a*-PCL-*ss*-Br with isobutyryl bromide end group (1.81g, yield: 61%).

Synthesis of diblock copolymer N_3-*a*-PCL-*ss*-PDMAEMA

Firstly, the diblock copolymer Cl-*a*-PCL-*ss*-PDMAEMA was synthesized by ATRP reaction of DMAEMA monomer using Cl-*a*-PCL-*ss*-Br as the macroinitiator in the presence of a CuBr/bpy catalyst system. In a 50 mL of dry flask, Cl-*a*-PCL-*ss*-Br (1.8 g, 0.26 mmol), CuBr (0.075 g, 0.52 mmol) and bpy (0.081 g, 0.52 mmol) were dissolved in 8 mL of anhydrous DMF under a dry nitrogen atmosphere. The mixture was degassed by three exhausting-refilling dry nitrogen cycles and a certain amount of DMAEMA (1.23 g, 7.8 mmol) was then injected into the flask by syringe. The polymerization was carried out at 50 °C for 24 h with continuous stirring and then quenched by exposing the mixture to air. The mixture was diluted with 100 mL of CH_2Cl_2 and passed through a column of basic alumina to remove the copper catalyst. Finally, the solution was concentrated and precipitated twice in 150 mL of cold hexanes, the precipitates were then collected and dried under vacuum at 30 °C to a constant weight to afford Cl-*a*-PCL-*ss*-PDMAEMA (1.95 g, yield: 64.3%).

Subsequently, in another 50 mL of dry flask, Cl-*a*-PCL-*ss*-PDMAEMA (1.6 g, 0.13 mmol) and NaN_3 (0.0845 g, 1.3 mmol) were dissolved in 10 mL of DMF, and the reaction was conducted at 60°C for 40 h. The mixture was passed through a column of basic alumina to remove the salt. The solution was concentrated under vacuum, diluted with 50 mL of CH_2Cl_2, and washed twice with PBS buffer solution (pH 10.0). The combined organic phase was dried over anhydrous $MgSO_4$ for 2 h, the filtrate was then concentrated and precipitated twice into 150 mL of cold hexanes. The precipitates were then collected and dried under vacuum at 30 °C to a constant weight to give N_3-*a*-PCL-*ss*-PDMAEMA (0.91 g, yield: 55%).

Polymer Chemistry Accepted Manuscript

Synthesis of Propargyl-PEEP

The monopropargyl-terminated poly(ethylethylene phosphate) (Propargyl-PEEP) was prepared by ROP reaction of EOP monomer using propargyl alcohol as the initiator and $Sn(Oct)_2$ as the catalyst. Briefly, a 50 mL of dry flask containing 15 mL of anhydrous THF was charged with propargyl alcohol (0.034 g, 0.6 mmol), EOP (2.47 g, 0.016 mol) and $Sn(Oct)_2$ (0.122 g, 0.3 mmol). The flask was degassed through three exhausting-refilling dry nitrogen cycles, and the reaction was carried out at 35 °C for 3 h with continuous stirring. Afterwards, the mixture was concentrated and precipitated twice in cold diethyl ether, the viscous product was then dried under vacuum at 25 °C to a constant weight (2.15 g, yield: 86%).

Synthesis of targeted reduction and pH dual-responsive triblock terpolymer Gal-PEEP-*a*-PCL-*ss*-PDMAEMA

Firstly, the disulfide and acetal-containing triblock terpolymer PEEP-*a*-PCL-*ss*-PDMAEMA was synthesized by CuAAC "click" reaction between Propargyl-PEEP and N_3-*a*-PCL-*ss*-PDMAEMA, and the typical procedure is listed below: In a 50 mL of dry flask, N_3-*a*-PCL-*ss*-PDMAEMA (0.8 g, 0.065 mmol), PMDETA (22.5 mg, 0.13 mmol) and Propargyl-PEEP (0.357 g, 0.07 mmol) were dissolved in 10 mL of anhydrous DMF, which were then degassed by three exhausting-refilling dry nitrogen cycles. Subsequently, CuBr (0.0186 g, 0.13 mmol) was added into the flask under a protection of dry nitrogen, and the solution was degassed once again and stirred at 25 °C for 24 h. After exposing the mixture to air to terminate the reaction and removing DMF under vacuum, the mixture was diluted with 100 mL of CH_2Cl_2 and passed through a column of basic alumina to remove the copper catalyst. The solution was then concentrated and dialyzed (MWCO 20000) against CH_2Cl_2 over two days, and the product was finally obtained by removing the solvent under vacuum (0.71 g, yield: 61%).

Subsequently, in another 50 mL of dry flask, PEEP-*a*-PCL-*ss*-PDMAEMA (0.5 g, 0.035 mmol) and CDI (0.0567 g, 0.35 mmol) were dissolved in 10 mL of anhydrous DMSO. The solution was stirred for 12 h at 25 °C, and then D-(+)-galactosamine hydrochloride (0.01 g, 0.046 mmol) and TEA (0.006 g, 0.058 mmol) in 5 mL of anhydrous DMSO was added dropwise to the activated polymer solution, and the reaction was carried out at 25 °C for 24 h. The mixture was then dialyzed (MWCO 20000) against CH_2Cl_2 over two days, and the product was finally obtained by removing the solvent under vacuum (0.26 g, yield: 50%).

Synthesis of PEEP-*b*-PCL-*b*-PDMAEMA triblock terpolymer without acetal and disulfide linkages

For comparison with Gal-PEEP-*a*-PCL-*ss*-PDMAEMA, we have synthesized another triblock terpolymer PEEP-*b*-PCL-*b*-PDMAEMA without acetal and disulfide linkages *via* a combination of ROP and ATRP reactions. Firstly, bifunctional initiator 2-hydroxyethyl 2-bromoisobutyrate (HEBI)[59] (0.1 g, 0.47 mmol), $Sn(Oct)_2$ (0.095 g, 0.24 mmol) and anhydrous toluene (20 mL) were charged into a 50 mL of dry flask under a dry nitrogen atmosphere. The mixture was degassed by three exhausting-refilling dry nitrogen cycles and ε-CL (2.68 g, 23.5 mmol) was then injected into the flask by syringe. The polymerization was allowed to proceed at 90 °C for 12 h. After that, the solution was concentrated and precipitated twice into 100 mL of cold diethyl ether, the white powder was then collected and dried under vacuum at 25 °C for 24 h to obtain HO-PCL-Br (1.97 g, yield: 71%).

Secondly, the diblock copolymer PEEP-*b*-PCL-Br with isobutyryl bromide end group was obtained by ROP reaction of EOP monomer using HO-PCL-Br as the marcoinitiator. Briefly, HO-PCL-Br (1.5 g, 0.224 mmol), $Sn(Oct)_2$ (0.05 g, 0.12 mmol) and anhydrous THF (20 mL) were sequentially added into a 50 mL of dry flask under a dry nitrogen atmosphere. The mixture was degassed by three exhausting-refilling dry nitrogen cycles and EOP (1.27 g, 7.9 mmol) was then added into the flask by syringe. The reaction was stirred at 40 °C for 5 h. After that, the solution was concentrated and precipitated twice into 100 mL of cold diethyl ether. The products PEEP-*b*-PCL-Br were isolated by filtration and drying under vacuum at 25 °C for 24 h (1.67 g, yield: 60%).

Finally, the triblock terpolymer PEEP-*b*-PCL-*b*-PDMAEMA was prepared by ATRP reaction of DMAEMA using PEEP-*b*-PCL-Br as the marcoinitiator. In a 50 mL of dry flask, PEEP-*b*-PCL-Br (1.5 g, 0.133 mmol), CuBr (0.0383 g, 0.266 mmol) and bpy (0.0415 g, 0.266 mmol) were dissolved in 10 mL of anhydrous DMF, followed by three exhausting-refilling dry nitrogen cycles. DMAEMA (0.63 g, 3.99 mmol) was then added into the flask by syringe, and the reaction was performed at 50 °C for 24 h. After that, DMF was removed under vacuum and the mixture was diluted with 200 mL of CH_2Cl_2 and passed through a column of basic alumina to remove the copper catalyst. The solution was concentrated and precipitated into 100 mL of cold hexanes/diethyl ether (*v*/*v* = 10/1). The precipitates were then collected and dried under vacuum at 25 °C for 24 h to afford the final product PEEP-*b*-PCL-*b*-PDMAEMA (1.06 g, yield: 50%).

Characterization

^{1}H NMR spectra were obtained by a NMR spectrometer (INOVA-400, Varian) at 25 °C using $CDCl_3$ as the solvent and TMS as the internal reference. FT-IR spectra were recorded on a Nicolet 6700 spectrometer using the KBr disk method. The number-averaged molecular weights and molecular weight distributions (PDIs) of polymers were measured on a Waters 1515 GPC instrument with a Waters 1515 isocratic HPLC pump, a Waters 2414 refractive index detector, a Waters 717 plus autosampler and a set of MZ-Gel SD plus columns (300 × 8.0 mm, 500 Å, 10^3 Å, and 10^4 Å). GPC measurements were carried out at 40 °C using DMF with 0.05 mol L^{-1} LiBr as eluent and the flow rate was 0.8 mL min^{-1}. The calibration was carried out with a series of polystyrene standards.

Self-assembly behavior of polymers

The critical aggregation concentration (CAC) values of the polymers in PBS buffer solution (pH 7.4) were investigated by the fluorescence probe method using pyrene as a hydrophobic probe. A predetermined amount of pyrene in acetone was added into a series of ampoules, and acetone was completely removed under vacuum. 5 mL of the polymer solutions with various concentrations were then added to each ampoule with the concentration of pyrene in each ampoule kept at 6×10^{-6} mol L^{-1}. The solutions were stirred at 25 °C for 24 h to reach equilibrium.

Polymer Chemistry Accepted Manuscript

This journal is © The Royal Society of Chemistry [year]

The fluorescence spectra were recorded on a spectrofluorometer (FLS920, Edinburgh). The excitation was carried out at 335 nm and the emission spectra were recorded ranging from 350 to 500 nm with both slit width for excitation and emission set at 1 nm. From the emission spectra of pyrene, the intensity ratios (I_3/I_1), namely, the third peak (383 nm, I_3) to the first peak (372 nm, I_1), were recorded as a function of polymer concentrations. The CAC value was defined as the point of intersection of the two lines in the plot of fluorescence versus polymer concentration.

The morphologies of the self-assembled micelles were observed on a TEM instrument (HT7700, Hitachi) operating at an accelerating voltage of 120 kV. Samples with a concentration of 0.4 mg mL^{-1} were prepared by the dialysis method. Typically, 10 mg of polymer was dissolved in 2 mL of DMSO and the solution was stirred for 4 h to ensure complete dissolution. 20 mL of Milli-Q water was then added dropwise to the solution over 12 h under vigorous stirring, followed by dialysis (MWCO 12000) against Milli-Q water for 24 h. After that, the solution was transferred to a volumetric flask, diluted with Milli-Q water to 25 mL, and stirred for 24 h before use. The sample for TEM analysis was then prepared by a freeze-drying method as described previously.[60] The carbon-coated copper grid was placed on the bottom of a glass cell, which was immediately inserted into liquid nitrogen. Subsequently, 20 μL of the micelle solution was dripped onto the grid, and the solvent in its frozen solid state was directly removed without melting in a freeze-drier. The morphology was imaged in a normal TEM instrument at room temperature.

The average particle sizes ($\overline{D}_z$) and size polydispersity indices (size PDIs) of the micelles were measured by a DLS instrument (Zetasizer Nano ZS, Malvern) at 25 °C. All samples were prepared by the same method as described in the TEM analysis and passed through a Φ0.45 μm microfilter before measurement. The size change of the micelles in different buffer solutions (pH 5.0, pH 5.0 with 10 mM GSH, and pH 7.4 with 10 mM GSH) were also measured by DLS analysis. Briefly, 2 mL of micelle solution (0.4 mg mL^{-1}) was adjusted to pH 5.0 or pH 7.4 with/without 10 mM GSH and incubated at 25 °C. At different time intervals, the average particle sizes were determined by DLS.

Agarose gel electrophoresis

The DNA condensation ability of Gal-PEEP-*a*-PCL-*ss*-PDMAEMA was investigated by gel retardation assay. The polyplex solution with different N/P ratios ranging from 0 to 12 was mixed with 2 μL of loading buffer (85% glycerol and 15% bromophenol blue) and run on a 0.8 wt% agarose gel with ethidium bromide (EB, 0.5 μg mL^{-1}) staining in Tris-borate-EDTA buffer solution (TBE: 40 mM trisborate, 1 mM EDTA, and pH 7.4). The retardation assays were performed at a voltage of 90 V for 30 min. The gel was visualized by a UV irradiation instrument (M-15E, UVP Inc.) to show the location of DNA.

Competitive binding assays and reduction-triggered unpacking of polyplexes

The competitive binding assays were performed using negatively-charged dextran sodium sulfate (DSS, $\overline{M}_w \approx 500000$ g mol^{-1}). Under a dry nitrogen atmosphere, a predetermined amount of GSH was added to 2 mL of terpolymer/DNA polyplexes prepared as described above to reach a final GSH concentration of 10 mM. After 1 h of incubation at 25 °C, DSS was added into polyplexes to give varying DSS/DNA charge ratios from 2 to 12. After further incubating at 25 °C for 30 min, the polyplexes were electrophoresed through a 0.8% agarose gel containing EB at 90 V in TBE buffer solution.

***In vitro* drug loading and release**

The DOX-loaded micelles were prepared as follows: DOX·HCl was first neutralized with excess amount of TEA to form free DOX before loading. 25 mg of triblock terpolymer was dissolved in 2 mL of DMSO and stirred at 25 °C for 4 h, followed by mixing with 250 μL of DOX/DMSO stock solution (18.7 mg mL^{-1}). Subsequently, 15 mL of Milli-Q water was added dropwise to the solution under vigorous stirring, and the solution was dialyzed (MWCO 7000) against Milli-Q water for 48 h to remove DMSO and unloaded DOX. During the process, the Milli-Q water was refreshed for several times at appropriate intervals. Finally, the DOX-loaded micelle solution was then diluted with 50 mL of Milli-Q water to a desired concentration. For the determination of DOX loading content, 5 mL of DOX-loaded micelle solution was lyophilized and dissolved in 5 mL of DMF. The solution was measured by fluorescence spectroscopy with excitation at 480 nm and emission at 590 nm, and the slit width was set at 5 nm. The concentration of DOX was calculated according to a calibration curve. The DOX loading content (DLC) and DOX loading efficiency (DLE) were calculated according to the following equations:

$$\text{DLC (\%)} = \frac{\text{Weight of DOX loaded in micelles}}{\text{Weight of polymer}} \times 100$$

$$\text{DLE (\%)} = \frac{\text{Weight of DOX loaded in micelles}}{\text{Weight of DOX in feed}} \times 100$$

The *in vitro* release of DOX experiments were performed at 37 °C in PB (pH 7.4 or pH 5.0, in the presence or absence of 10 mM GSH) with constant shaking. In brief, 5 mL of DOX-loaded micelle solution was placed in a dialysis bag (MWCO 7000), which was immersed in 20 mL of buffer solution incubated at 37 °C with continuous shaking. At the desired time intervals, 5 mL of the released medium was withdrawn for fluorescence analysis and 5 mL of corresponding fresh buffer was added to keep a constant volume. All the loading and release experiments were carried out in dark, and the release experiments were conducted in triplicate.

Cell culture

HeLa cells and HepG2 cells were purchased from American Type Culture Collection (ATCC). The cells were cultured in DMEM medium containing 10% heat-inactivated fetal bovine serum (FBS) and 1% penicillin/streptomycin solution at 37 °C under 5% CO_2 atmosphere, and used in their growth state. The culture media were replaced every three days.

***In vitro* cytotoxicity tests**

A standard methyl thiazolyl tetrazolium (MTT) assay was used to evaluate the cytotoxicity of the blank micelles and DOX-loaded micelles against HeLa cells and HepG2 cells, using free DOX as the control. Cells were seeded in a 96-well plate at a density of about 5×10^4 cells per well for 12 h. The sample solutions with different concentrations were then added to the wells and cultured

Polymer Chemistry Accepted Manuscript

for another 48 h. Afterwards, 25 μL of MTT stock solution (5 mg mL^{-1} in PBS) was added to each well. After incubation for another 4 h, DMEM medium was removed and the produced purple formazan was dissolved by adding 150 μL of DMSO. The optical density (OD) at 570 nm of each well was measured on a microplate reader (Bio-Rad 680). The absorbance values were normalized to the wells in which cells were not treated with samples. The cell viability was calculated by the equation of $OD_{sample}/OD_{control} \times 100\%$, in which OD_{sample} and $OD_{control}$ are the absorbance values of the testing well (in the presence of samples) and the control well (in the absence of samples), respectively. Data are presented as the average values with standard deviations.

Cellular uptake

The cellular uptake trials of DOX-loaded micelles against HeLa cells and HepG2 cells were performed on a live cell imaging system (CELL'R, Olympus). The cells were seeded onto *Φ*35 mm glass bottom culture dishes at a density of 2×10^4 cells cm^{-2}. After 12 h of incubation, the culture medium was removed. Cells were washed with PBS and stained with H 33342 (10 mg L^{-1}) for 15 min. Afterwards, the cells were incubated with DMEM medium containing DOX-loaded micelles (0.3 mg L^{-1} of DOX) at 37 °C under 5% CO_2 atmosphere during observation. Images were then captured at every 30 min with an excitation wavelength of 480 nm (red) and 340 nm (blue) for 24 h. The cells treated with free DOX (0.3 mg L^{-1}) were used as the control.

For flow cytometry analysis, HeLa cells and HepG2 cells were seeded onto *Φ*35 mm cell culture dishes at a density of 2×10^4 cells cm^{-2} and allowed to adhere for 12 h. Subsequently, the culture medium was replaced by 1.5 mL of fresh medium containing Gal-$PEEP_{33}$-*a*-PCL_{57}-*ss*-$PDMAEMA_{28}$/DOX (0.3 mg L^{-1} of DOX). After incubation at 37 °C for different time, the culture medium was removed, cells were then washed with PBS for three times and digested with trypsin. After that, 0.5 mL of culture medium was added to each culture dish, and the solutions were centrifuged at 1000 rpm for 3 min. After removal of the supernatants, the cells were resuspended in 0.5 mL of PBS. The fluorescence histograms of DOX in cells was recorded using a flow cytometry (Cytomics FC500, Beckman Coulter).

***In vitro* transfection**

In vitro transfection was performed against HeLa cells and HepG2 cells, which were seeded onto 35-mm glass bottom culture dishes at a density of 2×10^4 cells cm^{-2}. The blank terpolymer micelles and DOX-loaded terpolymer micelles were respectively mixed with the solution of DNA encoded with green fluorescence protein (GFP) at different N/P ratios in DMEM medium. They were further incubated at 25 °C for 30 min to allow the formation of terpolymer/DNA polyplexes or terpolymer/DOX/DNA polyplexes. Subsequently, 100 μL of the samples was added to each well and gently mixed by rocking the plate back and forth, which were further incubated for 6 h at 37 °C under 5% CO_2 atmosphere. After that, the samples were removed and 150 μL of fresh DMEM medium containing 10% serum was added. The cells were then incubated at 37 °C in a CO_2 incubator for 48 h. Finally, the transfection of complexes was visualized by a live cell imaging system, and the GFP expressing efficiency was measured by flow cytometry.

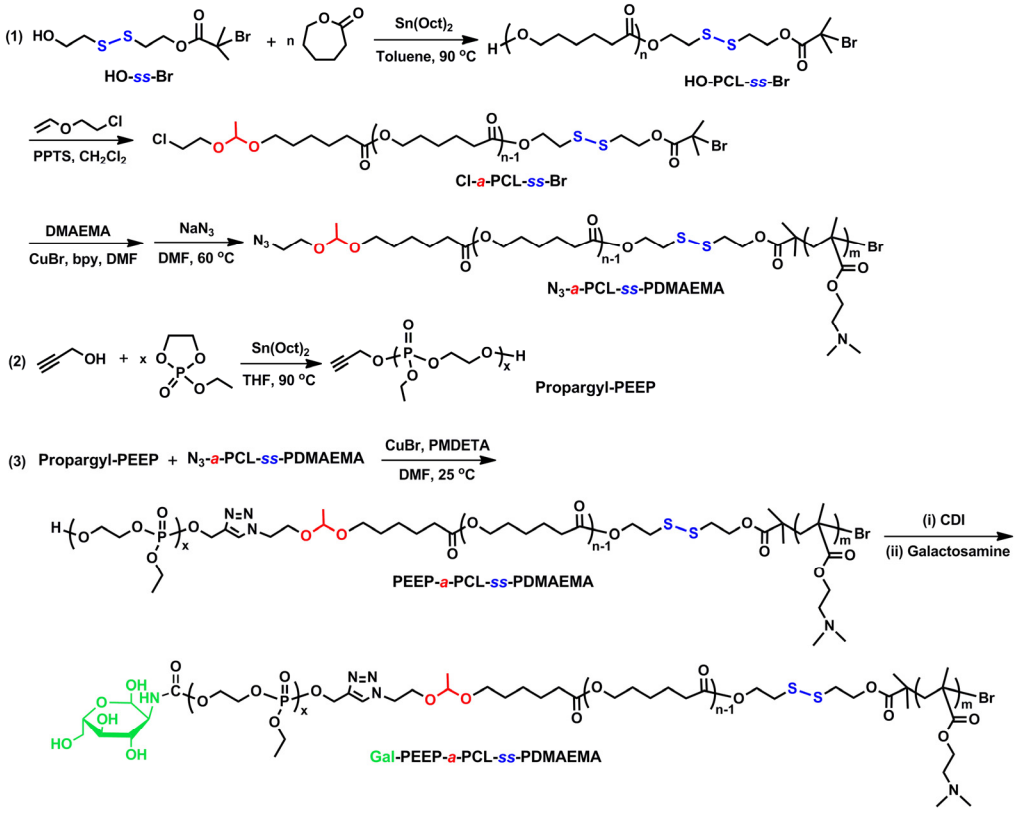

Scheme 2 Synthesis routes of reduction and pH dual-responsive triblock terpolymer conjugated with galactosamine Gal-PEEP-*a*-PCL-*ss*-PDMAEMA.

Polymer Chemistry Accepted Manuscript

This journal is © The Royal Society of Chemistry [year]

Results and discussion

Synthesis and characterization of Gal-PEEP-*a*-PCL-*ss*-PDMAEMA

The targeted reduction and pH dual-responsive triblock terpolymer Gal-PEEP-*a*-PCL-*ss*-PDMAEMA was prepared by several steps including ROP, ATRP, CuAAC, and polymer reactions, as illustrated in Scheme 2.

Firstly, a trifunctional polymer precursor N_3-*a*-PCL-*ss*-PDMAEMA was synthesized, in which the acetal, disulfide and clickable azide groups were integrated in one polymer chain. HO-*ss*-Br was employed to initiate the ROP reaction of ε-CL under the catalysis of $Sn(Oct)_2$ to produce HO-PCL-*ss*-Br; Subsequently, the acetal group was bonded to HO-PCL-*ss*-Br by reacting with CEVE using PPTS as the catalyst; After that, the diblock copolymer N_3-*a*-PCL-*ss*-PDMAEMA was prepared *via* ATRP reaction of DMAEMA using Cl-*a*-PCL-*ss*-Br as the macroinitiator followed by the nucleophilic substitution with NaN_3. Fig. 1 shows the ^{1}H NMR spectra of HO-*ss*-Br, HO-PCL_{57}-*ss*-Br, and Cl-*a*-PCL_{57}-*ss*-Br, respectively. All the characteristic peaks ascribed to the protons in the samples can be found in the spectra. It is worth noting that comparing with the spectrum of HO-PCL_{57}-*ss*-Br in Fig. 1(B), the spectrum of Cl-*a*-PCL_{57}-*ss*-Br exhibits new chemical shifts attributed to the protons of the acetal moiety (peaks h and i) as shown in Fig. 1(C). While for the spectrum of N_3-*a*-PCL_{57}-*ss*-$PDMEMA_{28}$ depicted in Fig. 2(A), except for the signals ascribed to the protons in PCL block (peaks c, d, e and f) which are consistent with the chemical shifts in Fig. 1(C), one can also find some new peaks (peaks l, m, p, q and r) attributed to the protons in PDMAEMA block. Moreover, FT-IR measurement was also used to characterize the diblock polymer and the result is shown in Fig. S1(A) in the ESI†. The appearance of the absorption peak at about 2109 cm^{-1} further indicated that the azide group have been successfully introduced to the end of diblock polymer.

Secondly, Propargyl-PEEP was synthesized by ROP reaction of EOP in the presence of propargyl alcohol and catalysis of $Sn(Oct)_2$. As shown in Fig. 2(B), one can find the characteristic signals of the methylene (peak y) and alkynyl protons (peak z) in the terminal propargyl group, and some other peaks ascribed to the PEEP block can also be found.

Finally, the targeted stimuli-responsive triblock terpolymer Gal-PEEP-*a*-PCL-*ss*-PDMAEMA was prepared by a two-step reaction: (i) first CuAAC "click" reaction betwee N_3-*a*-PCL-*ss*-PDMAEMA and Propargyl-PEEP; and (ii) conjugation with galactosamine using CDI as the coupling reagent. Fig. 2(C) shows the ^{1}H NMR spectrum of Gal-$PEEP_{33}$-*a*-PCL_{57}-*ss*-$PDMAEMA_{28}$, from which one can find that in addition to the proton signals of N_3-*a*-PCL_{57}-*ss*-$PDMAEMA_{28}$ and Propargyl-$PEEP_{33}$, the spectrum displays some characteristic signals resulting from the triazole ring at δ 7.84 ppm (peak z′) and glucosyl protons at δ 3.3-3.8 ppm, demonstrating the successful synthesis of Gal-$PEEP_{33}$-*a*-PCL_{57}-*ss*-$PDMAEMA_{28}$. Besides, as shown in Fig. S1(C) in the ESI,† the chemical shifts attributed to azide group completely disappeared while the peaks of the carbonyl group and some groups from PEEP segment maintained after the "click" reaction, which further confirmed the successful synthesis of triblock terpolymer. Furthermore, the residual Cu

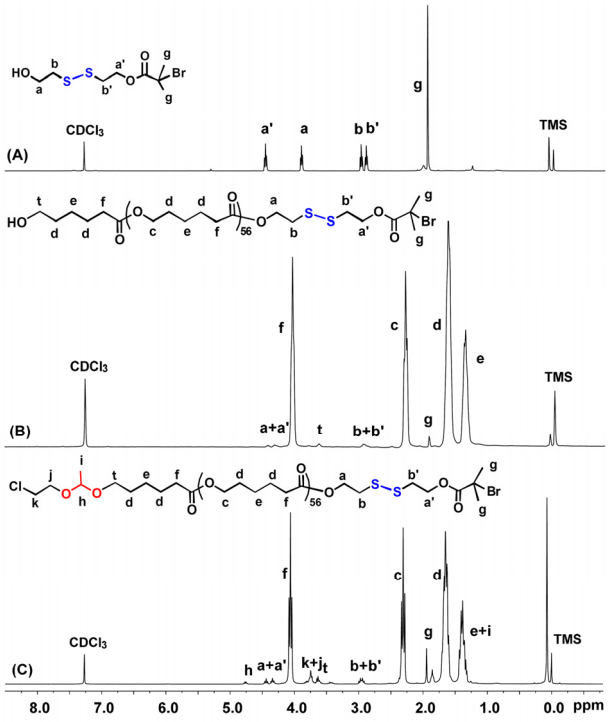

Fig. 1 ^{1}H NMR spectra of (A) HO-*ss*-Br, (B) HO-PCL_{57}-*ss*-Br, and (C) Cl-*a*-PCL_{57}-*ss*-Br.

content in the terpolymer was measured by atomic absorption spectrometry and shown about 0.12 ppm, indicating that most of the copper catalyst was removed during the dialysis process.

For simplicity, HO-PCL_n-*ss*-Br, HO-PCL_n-*ss*-$PDMAEMA_x$, Propargyl-$PEEP_m$, and $PEEP_m$-*a*-PCL_n-*ss*-$PDMAEMA_x$ were abbreviated as C_n, C_n-*ss*-D_X, E_m, and E_m-*a*-C_n-*ss*-D_x, respectively. The number-averaged molecular weights ($\overline{M}_{n,NMR}$) of various polymers were first calculated by the eqn (1)~(4) according to the integral values of characteristic peaks in ^{1}H NMR spectra, where *A* represents the integral values of peaks; the subscripts of g, e, w, q and y are corresponding to the peaks in ^{1}H NMR spectra.

$$n = \frac{3A_e}{A_g};\quad \overline{M}_{n,NMR(C_n)} = n \times 114.1 + 303.2 \qquad (1)$$

$$m = \frac{2A_w}{3A_y};\quad \overline{M}_{n,NMR(E_m)} = m \times 152.1 + 56.1 \qquad (2)$$

$$x = \frac{A_q}{A_e} \times n;\quad \overline{M}_{n,NMR(C_n\text{-}ss\text{-}D_X)} = x \times 157.2 + \overline{M}_{n,NMR(C_n)} \qquad (3)$$

$$\overline{M}_{n,NMR(E_m\text{-}a\text{-}C_n\text{-}ss\text{-}D_x)} = \overline{M}_{n,NMR(C_n\text{-}ss\text{-}D_X)} + \overline{M}_{n,NMR(E_m)} \qquad (4)$$

where 303.2 is the molecular weight of HO-*ss*-Br initiator; 114.1, 152.1 and 157.2 are the molecular weights of ε-CL, EOP and DMAEMA monomers, respectively.

The number-averaged molecular weights ($\overline{M}_{n,GPC}$) and molecular weight distributions (PDIs) of polymers were measured by GPC analysis and the data are listed in Table 1. In addition, GPC traces of representative homopolymer, diblock copolymer and triblock terpolymer are illustrated in Fig. 3, in which all of them exhibit unimodal distribution, and no significant shoulder peaks are observed. Moreover, both of the traces of diblock copolymer and triblock terpolymer shift towards higher molecular weight side compared with that of homopolymer, indicating the growth of molecular weights and successful polymerization.

Polymer Chemistry Accepted Manuscript

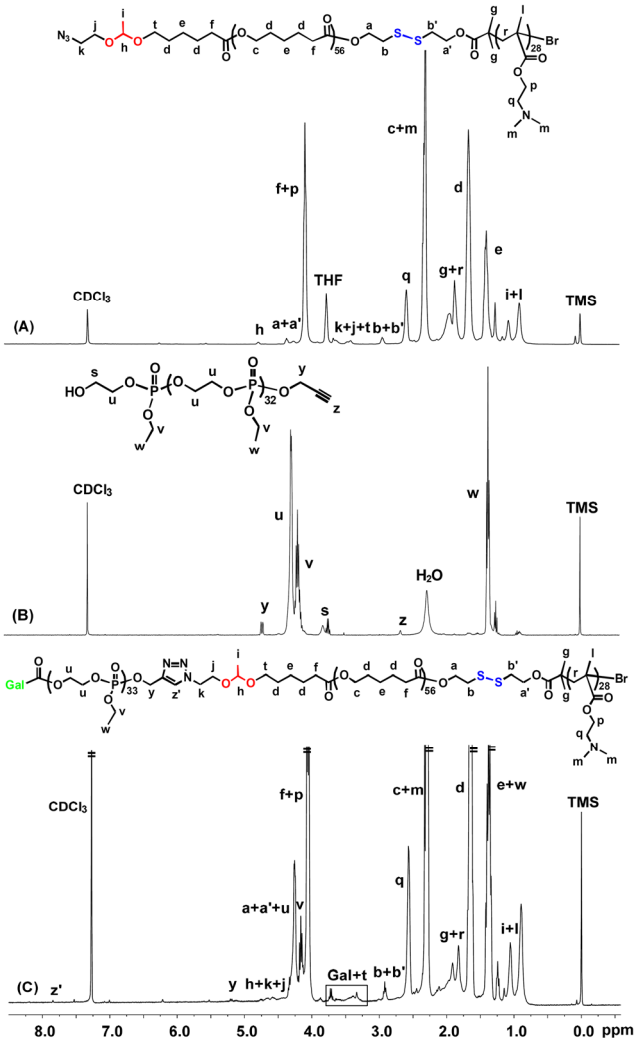

Fig. 2 ^{1}H NMR spectra of (A) N_3-*a*-PCL_{57}-*ss*-$PDMAEMA_{28}$, (B) Propargyl-$PEEP_{33}$, and (C) Gal-$PEEP_{33}$-*a*-PCL_{57}-*ss*-$PDMAEMA_{28}$.

Table 1 Characterization data of the compositions, number-average molecular weights and molecular weight distributions (PDIs) of various polymers.

Samples	$\overline{M}_{n,NMR}$ [a] (g mol^{-1})	$\overline{M}_{n,GPC}$ [b] (g mol^{-1})	PDI [b]
HO-PCL_{57}-*ss*-Br	6640	10020	1.10
Propargyl-$PEEP_{33}$	4690	9270	1.14
N_3-*a*-PCL_{57}-*ss*-$PDMAEMA_{28}$	12350	16090	1.17
N_3-*a*-PCL_{57}-*ss*-$PDMAEMA_{36}$	13580	16370	1.18
$PEEP_{33}$-*a*-PCL_{57}-*ss*-$PDMAEMA_{36}$	18460	27060	1.47
$PEEP_{33}$-*a*-PCL_{57}-*ss*-$PDMAEMA_{28}$	14280	20720	1.38
HO-PCL_{56}-Br	6520	9870	1.06
$PEEP_{30}$-PCL_{56}-Br	9850	11820	1.12
$PEEP_{30}$-*b*-PCL_{56}-*b*-$PDMAEMA_{25}$	12600	15500	1.15

[a] Calculated by eqn (1)~(4) based on ^{1}H NMR analysis. [b] Measured by GPC with DMF as the eluent and polystyrene as standards.

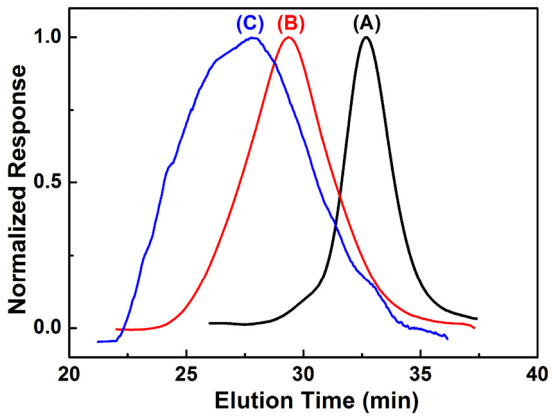

Fig. 3 GPC curves of (A) HO-PCL_{57}-*ss*-Br (C_{57}, $\overline{M}_{n,GPC}$ = 10020 g mol^{-1}, PDI = 1.10), (B) N_3-*a*-PCL_{57}-*ss*-$PDMAEMA_{28}$ (C_{57}-*ss*-D_{28}, $\overline{M}_{n,GPC}$ = 16090 g mol^{-1}, PDI = 1.17), (C) $PEEP_{33}$-*a*-PCL_{57}-*ss*-$PDMAEMA_{28}$ (E_{33}-*a*-C_{57}-*ss*-D_{28}, $\overline{M}_{n,GPC}$ = 20720 g mol^{-1}, PDI = 1.38).

Synthesis and characterization of triblock terpolymer PEEP-*b*-PCL-*b*-PDMAEMA without acetal and disulfide linkages

The synthesis route including a combination of two consecutive ROP reactions and one ATRP reaction towards the triblock terpolymer PEEP-*b*-PCL-*b*-PDMA without acetal and disulfide linkages is shown in Scheme S1 in the ESI†. ^{1}H NMR and GPC measurements were employed to characterize the chemical structures of various polymers. From the ^{1}H NMR spectrum in Fig. S2 in the ESI†, one can find all the chemical shifts ascribed to the corresponding protons of the terpolymer. GPC curves of HO-PCL_{56}-Br, $PEEP_{30}$-*b*-PCL_{56}-Br and $PEEP_{30}$-*b*-PCL_{56}-*b*-$PDMAEMA_{25}$, as shown Fig. S3 in the ESI†, display that the terpolymer has a unimodal peak and shifts toward the side of higher molecular weight compared to the precurror, indicating the successful preparation of the desired triblock terpolymer.

Self-assembly behavior

It is widely recognized that amphiphilic copolymers can self-assemble into micelles in aqueous solution when the polymer concentration exceeds a critical value, which is defined as the critical aggregation concentration (CAC) value. Herein, the CAC value of triblock terpolymer was determined by pyrene fluorescence probe method, which was calculated from the plot of intensity ratios (I_3/I_1) as a function of the polymer concentrations. A series of triblock terpolymer solution with different concentrations were prepared and the I_3/I_1 ratios in fluorescence emission spectra of pyrene were recorded. The relationship of I_3/I_1 as a function of the logarithm concentrations is shown in Fig.S4 in the ESI†, from which the CAC value is determined to be 0.038 mg mL^{-1}. Furthermore, the micellization was further studied by TEM and DLS analyses. Fig. 4(A) shows the typical TEM image of micelles self-assembled from Gal-E_{33}-*a*-C_{57}-*ss*-D_{28} in aqueous solution (0.4 mg mL^{-1}), from which one can find that the micelles are spherical and the average size is less than 150 nm. The average particle sizes ($\overline{D}_z$) and size polydispersity indices (size PDIs) of the polymeric micelles are very important for drug carriers. A suitable size (< 200 nm in diameter) is optimum to minimize the uptake of nanoparticles by a reticuloendothelial system (RES), while holding the advantage of the EPR effect for passive targeting.[61] As shown in Fig. 4(B), the corresponding particle size distribution histogram of Gal-E_{33}-*a*-

Polymer Chemistry Accepted Manuscript

This journal is © The Royal Society of Chemistry [year]

C_{57}-*ss*-D_{28} micelles measured by DLS analysis displays a monomodal peak with an average diameter of 130 nm and size PDI of 0.201. The difference in average particle sizes determined from TEM and DLS analyses may be caused by the hydrophilic blocks, which can extend into the water phase during DLS measurement, but is hardly observed in dry state in TEM images. As a comparison, Fig. 4(C) and (D) show the TEM image and corresponding particle size distribution histogram of DOX-loaded Gal-E_{33}-*a*-C_{57}-*ss*-D_{28} micelles, respectively. Because the poorly water-soluble DOX was loaded into the hydrophobic core of micelles, which enhanced the size of the core and the average particle size of DOX-loaded micelles increased to about 169 nm.

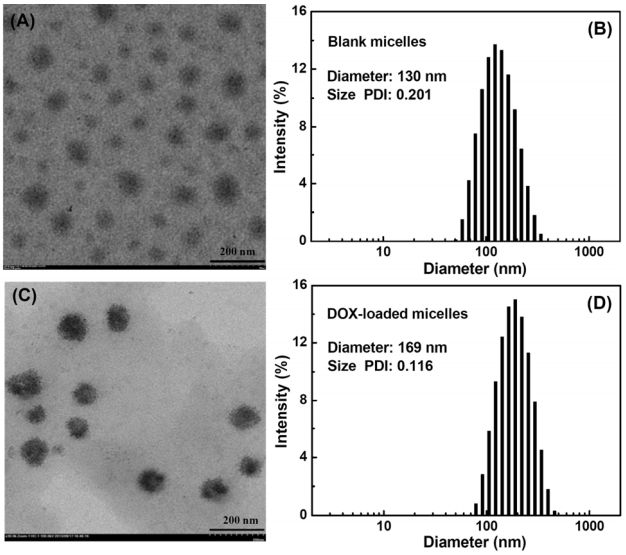

Fig. 4 TEM images of (A) blank micelles and (C) DOX-loaded micelles self-assembled from Gal-E_{33}-*a*-C_{57}-*ss*-D_{28}, scale bar = 200 nm; (B) and (D) are the particle size distribution histograms corresponding to the samples in (A) and (C), respectively.

Reduction and pH-induced size change of Gal-PEEP-*a*-PCL-*ss*-PDMAEMA micelles

The size change of Gal-E_{33}-*a*-C_{57}-*ss*-D_{28} micelles in response to acidic (pH 5.0) and reducing (10 mM GSH) conditions were studied by DLS analysis. As shown in Fig. 5(A), the size of micelles at the initial time was about 130 nm, and it increased gradually with the increase of incubation time in pH 5.0 buffer solutions. In addition, obvious size change of Gal-E_{33}-*a*-C_{57}-*ss*-D_{28} micelles was also observed at pH 7.4 in the presence of 10 mM GSH, where the size of micelles increased from about 130 nm to 350 nm in 24 h as shown in Fig. 5(B). More importantly, it can be clearly found from Fig. 5(C) that the fastest size change of micelles was discerned at pH 5.0 in the presence of 10 mM GSH, in which large aggregates with an average diameter over 1000 nm were formed in 24 h. In comparison, it should be noted from Fig. 5(D) that no obvious size change was detected for reduction and pH-insensitive $PEEP_{30}$-*b*-PCL_{56}-*b*-$PDMAEMA_{25}$ micelles after 24 h of incubation under the same conditions. To further verify the degradation of terpolymer, we utilized GPC analysis to determine the molecular weights of the degradation products of Gal-E_{33}-*a*-C_{57}-*ss*-D_{28}. As shown in Fig. S5, both of the GPC traces of GSH-triggered and pH-triggered degradation products shift towards the sides of lower molecular weights compared with that of original terpolymer. These results confirmed the degradation of terpolymer micelles under the acidic and reducing conditions, and thus possibly inducing synergistic effects for triggered intracellular release of loaded cargos.

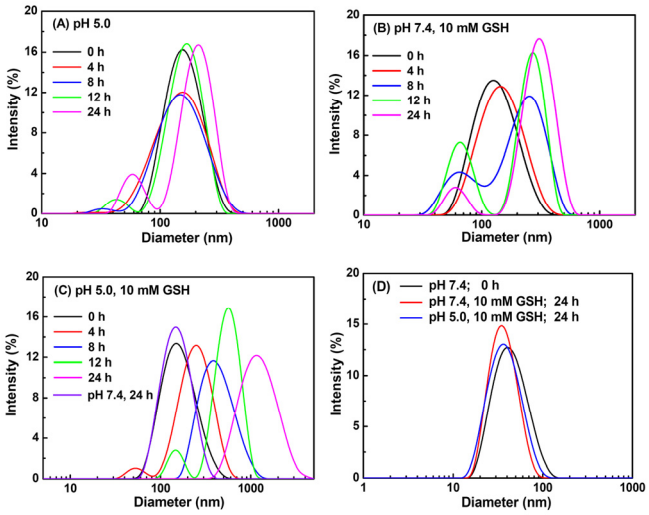

Fig. 5 (A), (B) and (C) are the curves of reduction and pH-induced size change of Gal-E_{33}-*a*-C_{57}-*ss*-D_{28} micelles monitored by DLS at different conditions; (D) is the size change of $PEEP_{30}$-*b*-PCL_{56}-*b*-$PDMAEMA_{25}$ micelles monitored by DLS at different conditions.

In vitro loading and release of DOX

Herein, DOX was chosen as the hydrophobic model drug because it is one of the most widely applied anticancer drugs for the treatment of various solid malignant tumors in the clinics, and its intrinsic red fluorescence provides more convenience to observe the cellular uptake and intracellular release behavior. DOX was respectively loaded into Gal-E_{33}-*a*-C_{57}-*ss*-D_{28} and $PEEP_{30}$-*b*-PCL_{56}-*b*-$PDMAEMA_{25}$ micelles by a dialysis method. The drug loading content (DLC) and drug loading efficiency (DLE) of Gal-E_{33}-*a*-C_{57}-*ss*-D_{28} micelles were determined by fluorescence measurement to be 5.1% and 15.3%, while the DLC and DLE values for $PEEP_{30}$-*b*-PCL_{56}-*b*-$PDMAEMA_{25}$ micelles were 6.1% and 12.5%. The *in vitro* release of DOX from DOX-loaded Gal-E_{33}-*a*-C_{57}-*ss*-D_{28} micelles were carried out at 37 °C under different conditions, *i.e.* (i) pH 7.4, (ii) pH 5.0, (iii) pH 7.4 in the presence of 10 mM GSH, and (iv) pH 5.0 in the presence of 10 mM GSH. The cumulative release profiles of DOX from the micelles are shown in Fig. 6(A), from which one can observe that only about 21% of DOX was released after 48 h of incubation at pH 7.4, while the released DOX was about 96% at pH 5.0 under the same condition, much higher than that at pH 7.4. These results could be attributed to pH-induced acetal cleavage.[18,19,26] Similarly, the release of DOX was accelerated under a reducing condition of 10 mM GSH at pH 7.4, from which about 95% of DOX was also released in 48 h. This reduction-triggered drug release behavior has been reported for different copolymer micelles.[32,34,35] Remarkably, the fastest and most complete release of DOX was observed at pH 5.0 in the presence of 10 mM GSH. In this case, there was about 98% of DOX released in 10 h. This is in accordance with the observation in Fig. 5(C), which described the rapid dissociation of Gal-E_{33}-*a*-C_{57}-*ss*-D_{28} micelles at the condition of pH 5.0 with 10 mM GSH. It is very important

Polymer Chemistry Accepted Manuscript

for the responsive copolymer micelles to hold enhanced stability of at pH 7.4 because most of DOX will not be released during blood circulation and thus avoiding some side effects of DOX to normal tissues. In comparison, the release of DOX from DOX-loaded $PEEP_{30}$-*b*-PCL_{56}-*b*-$PDMAEMA_{25}$ micelles without acetal and disulfide linkages was also investigated as the control, and the DOX-loaded micelles were prepared as described for Gal-E_{33}-*a*-C_{57}-*ss*-D_{28} sample. As shown in Fig. 6(B), the release rates of DOX kept at a relatively low level and were not influenced in the presence of 10 mM GSH both at pH 5.0 and 7.4 conditions. Therefore, these results demonstrated that the reduction and pH dual-responsive Gal-E_{33}-*a*-C_{57}-*ss*-D_{28} micelles possess potential applications for the selective release of drugs under intracellular environments.

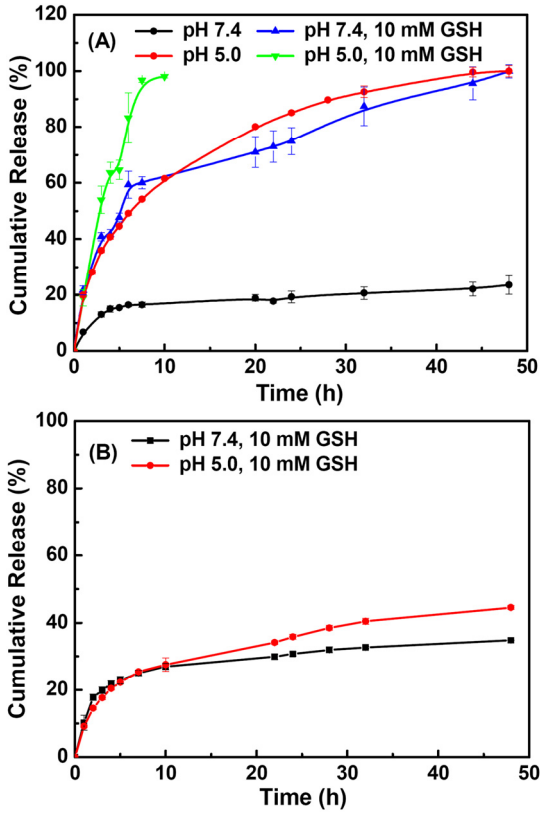

Fig. 6 (A) Release of DOX from DOX-loaded Gal-E_{33}-*a*-C_{57}-*ss*-D_{28} micelles at 37 °C at different conditions; (B) Release of DOX from DOX-loaded $PEEP_{30}$-*b*-PCL_{56}-*b*-$PDMAEMA_{25}$ micelles at 37 °C at different conditions.

In vitro cytotoxicity and cellular uptake of DOX-loaded micelles

Cytotoxicity is one of the important considerations in the design of gene or drug carriers, so the *in vitro* cytotoxicity of Gal-PEEP-*a*-PCL-*ss*-PDMAEMA triblock terpolymer against HeLa cells and HepG2 cells was evaluated by MTT assay in this work. As shown in Fig. 7, the Gal-E_{33}-*a*-C_{57}-*ss*-D_{28} micelles exhibited dose-dependent toxic effects with the increase of polymer concentrations. Meanwhile, the cytotoxicity of degradation products of Gal-E_{33}-*a*-C_{57}-*ss*-D_{28} triblock terpolymer was also measured and the results are shown in Fig. S6 in the ESI†, which showed a similar tendency as the terpolymer. In addition, the *in vitro* cytotoxicity of DOX-loaded terpolymer micelles against HepG2 cells and HeLa cells were also investigated by MTT assay. Fig. 8(A) is the cell viability of HepG2 cells incubated with DOX-loaded E_{33}-*a*-C_{57}-*ss*-D_{28} and $PEEP_{30}$-*b*-PCL_{56}-*b*-$PDMAEMA_{25}$ micelles at different DOX concentrations ranging from 0.625 to 10 mg L^{-1} for 48 h using free DOX as the control. One can find that DOX-loaded terpolymer micelles showed lower cytotoxicity against HepG2 cells compared with free DOX at the same dosages, which might because of the prolonged release of DOX from micelles as indicated by *in vitro* DOX release profile discussed above. Moreover, the dual-responsive E_{33}-*a*-C_{57}-*ss*-D_{28} micelles exhibited stronger inhibition of cell proliferation than $PEEP_{30}$-*b*-PCL_{56}-*b*-$PDMAEMA_{25}$ micelles. The IC_{50} values (inhibitory concentration that produces 50% cell death) of E_{33}-*a*-C_{57}-*ss*-D_{28} and $PEEP_{30}$-*b*-PCL_{56}-*b*-$PDMAEMA_{25}$ micelles are 6.3 and 9.3 mg of DOX equiv. L^{-1}, respectively. Subsequently, the effect of targeted Gal moieties on the inhibition of cell proliferation was investigated. Fig. 8(B) is the cell viability of HepG2 cells incubated with DOX-loaded Gal-E_{33}-*a*-C_{57}-*ss*-D_{28} and E_{33}-*a*-C_{57}-*ss*-D_{28} micelles at different DOX concentrations ranging from 0.625 to 10 mg L^{-1} for 48 h using free DOX as the control. One can clearly observe that DOX-loaded Gal-E_{33}-*a*-C_{57}-*ss*-D_{28} micelles exhibited much higher cytotoxicity against HepG2 cells compared with DOX-loaded E_{33}-*a*-C_{57}-*ss*-D_{28} micelles, for which the IC_{50} values are determined to be 1.6 and 6.3 mg of DOX equiv. L^{-1}, respectively. This result indicated that DOX could be more efficiently delivered into HepG2 cells with the assistance of Gal-mediated endocytosis. Furthermore, HeLa cells were also treated for 48 h with DOX-loaded Gal-E_{33}-*a*-C_{57}-*ss*-D_{28} micelles at the same DOX concentrations and the result is shown in Fig. 8(C). The result also demonstrated that DOX-loaded Gal-E_{33}-*a*-C_{57}-*ss*-D_{28} micelles possess a higher activity to inhibit the growth of HepG2 cells than HeLa cells, further supporting the enhancement by the specific interaction between DOX-loaded Gal-E_{33}-*a*-C_{57}-*ss*-D_{28} micelles and HepG2 cells.

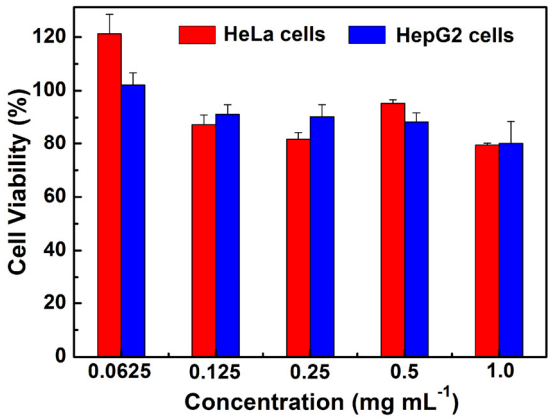

Fig. 7 Cell viability of HeLa cells and HepG2 cells incubated with Gal-E_{33}-*a*-C_{57}-*ss*-D_{28} micelles at various polymer concentrations for 48 h.

In order to investigate the intracellular release of DOX from DOX-loaded Gal-E_{33}-*a*-C_{57}-*ss*-D_{28} micelles, a live cell imaging system was employed and the release of DOX can be estimated by observing the red fluorescence intensity of DOX inside cells. Fig. 9 shows the fluorescence images of HepG2 cells and HeLa cells treated with DOX-loaded Gal-E_{33}-*a*-C_{57}-*ss*-D_{28} micelles, from which one can observe that the red fluorescence intensity of DOX in both cells became stronger with the increase of

Polymer Chemistry Accepted Manuscript

This journal is © The Royal Society of Chemistry [year]

incubation time, indicating that DOX was gradually released. More importantly, the red fluorescence intensity in HeLa cells was much weaker than that in HepG2 cells, demonstrating the easier internalization of DOX-loaded Gal-E_{33}-*a*-C_{57}-*ss*-D_{28} micelles by HepG2 cells *via* the receptor-mediated endocytosis. Furthermore, the result was verified by the flow cytometry displayed in Fig. S7 in the ESI†. One can find that the geometrical mean fluorescence intensities (GMFI) of HeLa cells were 8.29, 11.8, and 15.12 after incubation for 2 h, 5 h and 10 h, respectively, while the values of HepG2 cells were increased to 16.16, 19.06, and 22.72.

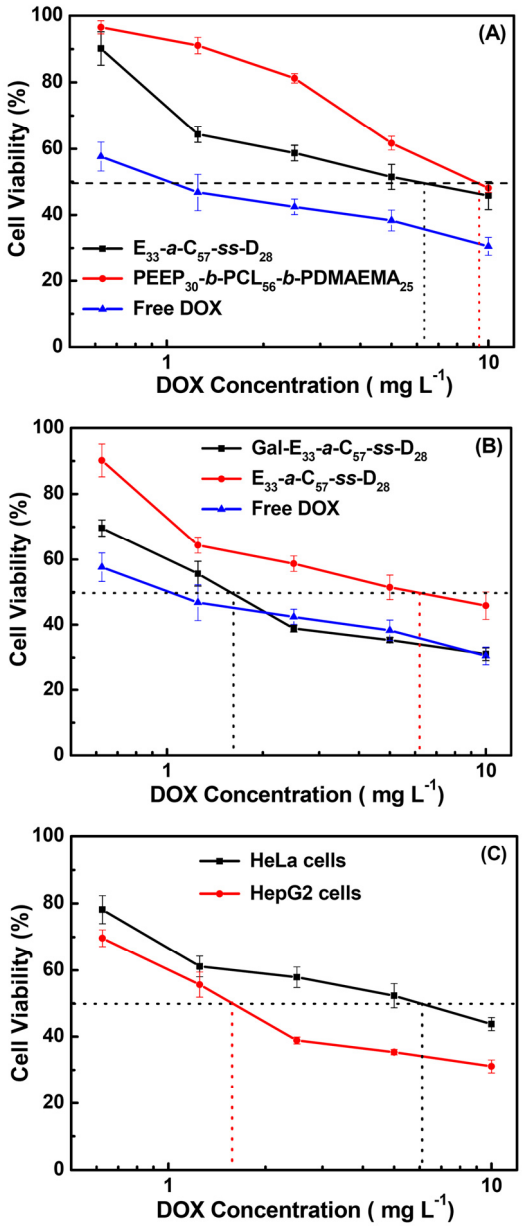

Fig. 8 (A) and (B) are the cell viability of HepG2 cells incubated with DOX-loaded terpolymer micelles and free DOX with different DOX concentrations for 48 h; (C) is the cell viability of HeLa cells and HepG2 cells incubated with DOX-loaded Gal-E_{33}-*a*-C_{57}-*ss*-D_{28} micelles with different DOX concentrations for 48 h.

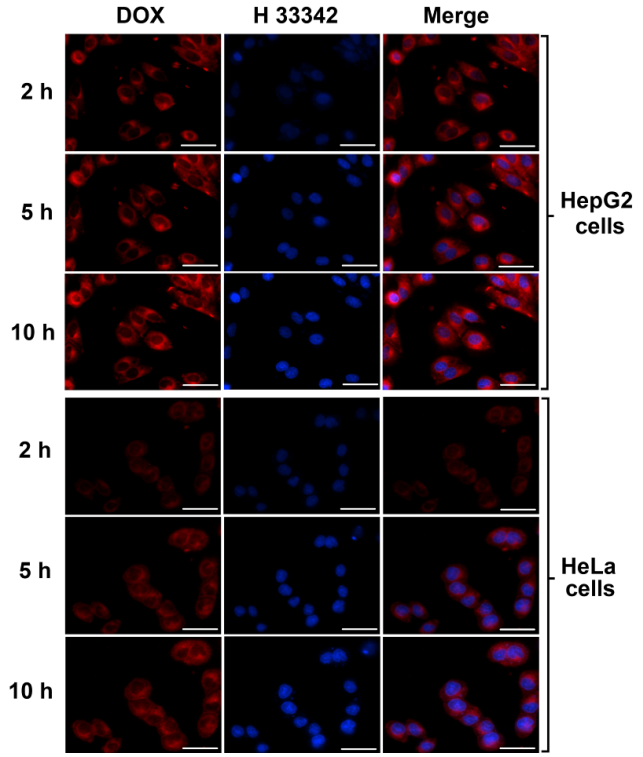

Fig. 9 Fluorescence images of HepG2 cells and HeLa cells treated with DOX-loaded Gal-E_{33}-*a*-C_{57}-*ss*-D_{28} micelles (final DOX concentration was 0.3 mg L^{-1}) for different incubation time. For each panel, the images from left to right show red fluorescence of DOX, nuclei stained by H 33342, and the overlays of two images. The scale bars correspond to 50 μm in all images.

Physical properties of terpolymer/DNA polyplexes

It is known that a good gene vector should effectively condense and protect DNA under extracellular conditions while efficiently deliver and release DNA inside cells. In this work, the binding capacity of these cationic terpolymers with DNA was first studied by agarose gel electrophoresis at various ratios of amino group in cationic terpolymer to phosphate group in DNA, defined as N/P ratios. Fig. 10 shows the agarose gel electrophoresis image of Gal-E_{33}-*a*-C_{57}-*ss*-D_{28}/DNA polyplexes at various N/P ratios. Lane 1 is the DNA control and it can migrate without any retardation. However, DNA migration could be gradually retarded with the increase of N/P ratios and the complete retardation of DNA can be observed when N/P ratio reached to 2 (lane 5). This result indicated that the protonated amine groups of PDMAEMA segment in the terpolymer could interact with the negatively-charged DNA to form the terpolymer/DNA polyplexes. In addition, reduction-triggered DNA release from Gal-E_{33}-*a*-C_{57}-*ss*-D_{28}/DNA polyplexes was also studied by gel retardation assays. Fig. 11 shows Gal-E_{33}-*a*-C_{57}-*ss*-D_{28}/DNA polyplexes formed at a N/P ratio of 15 were stable against 10-fold excess of negatively-charged dextran sodium sulfate (DSS), further confirming that the polyplexes were capable of strongly binding with DNA. However, release of DNA was clearly observed following incubation with 10 mM GSH under the same conditions, supporting that on one hand the polyplexes possess DNA condensation ability and colloidal stability, and on the other hand intracellular level of reducing condition might trigger unpacking of polyplexes.

Polymer Chemistry Accepted Manuscript

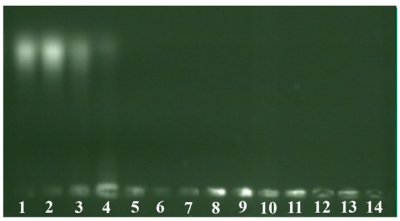

Fig. 10 Agarose gel electrophoresis of Gal-E_{33}-*a*-C_{57}-*ss*-D_{28}/DNA polyplexes prepared at various N/P ratios. Lane 1 is the DNA control; lane 2-14 correspond to N/P ratios of 0.1, 0.5, 1, 2, 3, 5, 7, 10, 15, 18, 20, 23 and 25, respectively.

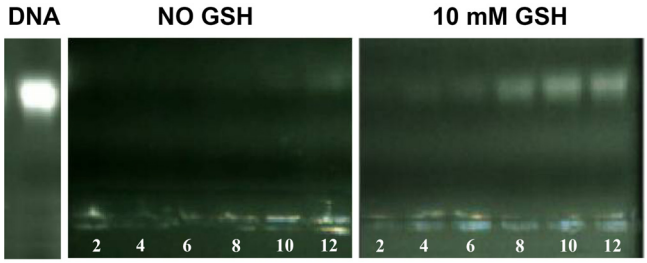

Fig. 11 Agarose gel electrophoresis of Gal-E_{33}-*a*-C_{57}-*ss*-D_{28}/DNA polyplexes formed at a N/P ratio of 15 following incubation with negatively-charged DSS at varying DSS/DNA charge ratios of 2, 4, 6, 8, 10 and 12 in the absence or presence of 10 mM GSH.

On the other hand, the zeta potential of Gal-E_{33}-*a*-C_{57}-*ss*-D_{28}/DNA complexes at various N/P ratios was tested and the result is shown in Fig. 12. The zeta potential of naked DNA was about -50 mV, and the values of polyplexes changed from a negative value to a positive one with the increase of N/P ratios. When the N/P ratio was higher than 2, DNA was fully neutralized with the cationic terpolymer to form the complexes with positive charge on the surface. These results were in line with the gel retardation electrophoresis results. Meanwhile, TEM and DLS analyses were also used to characterize the Gal-E_{33}-*a*-C_{57}-*ss*-D_{28}/DNA and Gal-E_{33}-*a*-C_{57}-*ss*-D_{28}/DOX/DNA polyplexes in aqueous solution at pH 7.4. Fig. 13(A) and (C) show the TEM images of terpolymer/DNA and terpolymer/DOX/DNA polyplexes at a N/P ratio of 15, while Fig. 13(B) and (D) are the corresponding particle size distribution histograms, respectively. One can find that the average particle size of polyplexes increased to about 158 nm after loading DNA, and this value further increased to about 198 nm after simultaneous loading DNA and DOX.

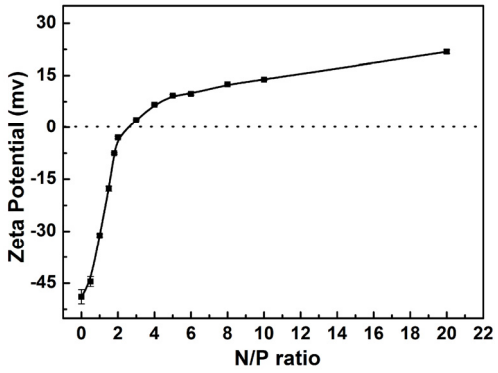

Fig. 12 Zeta potential of Gal-E_{33}-*a*-C_{57}-*SS*-D_{28}/DNA polyplexes at various N/P ratios.

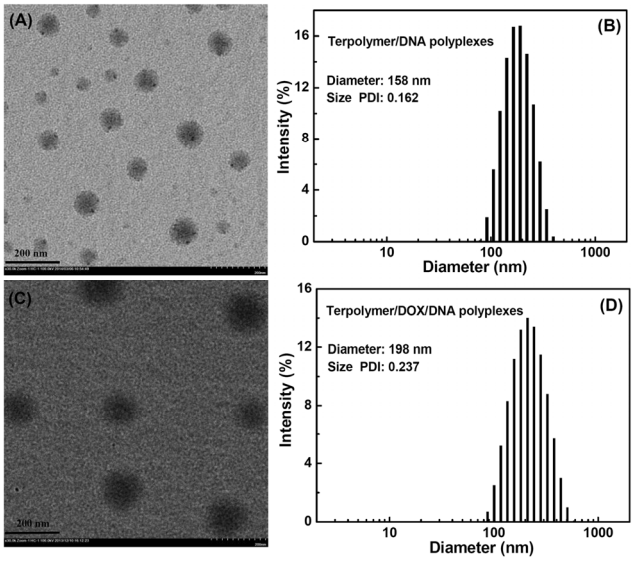

Fig. 13 TEM images of (A) terpolymer/DNA and (C) terpolymer/DNA/DOX polyplexes self-assembled from Gal-E_{33}-*a*-C_{57}-*ss*-D_{28} at a N/P ratio of 15, scale bar = 200 nm; (B) and (D) are the particle size distribution histograms corresponding to the samples in (A) and (C), respectively.

In vitro Simultaneous delivery of DNA and DOX

It was reported that the combinatorial delivery of chemotherapeutic drugs and genes in the same carrier would be a promising strategy for the treatment of cancers because the co-delivered therapeutic agents could exert a combined effect in the same cells.[37,38] As we described above, the present copolymer system with favorable biocompatibility and dual sensitivity can separately achieve the efficient loading and triggered release of DNA and DOX. Therefore, the co-delivery of GFP-DNA and DOX into both HepG2 cells and HeLa cells were investigated by a fluorescence microscopy and a flow cytometry. The DOX-loaded Gal-E_{33}-*a*-C_{57}-*ss*-D_{28} micelles were interacted with GFP-DNA *via* electrostatic interaction to form Gal-E_{33}-*a*-C_{57}-*ss*-D_{28}/GFP-DNA/DOX polyplexes. The fluorescence microscopy images shown in Fig. 14 clearly indicated that the fluorescence intensity for both HepG2 cells and HeLa cells became stronger with the increase of N/P ratio. Moreover, for HepG2 cells, a high degree of colocalization of the red and green fluorescence emitted by DOX and GFP can be observed for each N/P ratio, demonstrating that the efficient co-delivery of GFP-DNA and DOX into HepG2 cells. One can also find that the fluorescence intensity of both DOX and GFP in HepG2 cells is significantly stronger than that in HeLa cells at each N/P ratio, which was the result of specific interaction between Gal-E_{33}-*a*-C_{57}-*ss*-D_{28}/GFP-DNA/DOX polyplexes and ASGPRs-overexpressing HepG2 cells. In addition, the transfection efficiency of Gal-E_{33}-*a*-C_{57}-*ss*-D_{28}/GFP-DNA/DOX polyplexes in HepG2 cells and HeLa cells were tested by flow cytometry. As shown in Fig. 15, one can observe that for both HepG2 cells and HeLa cells, the expressing efficiency became higher with the increase of N/P ratio, which coincides with the enhancement of fluorescence intensity displayed in Fig. 14. The higher transfection efficiency of polyplexes into HepG2 cells than HeLa cells further proved that the Gal ligand attached on the surface of polyplexes plays a significant role to enhance the internalization into HepG2 cells.

Polymer Chemistry Accepted Manuscript

This journal is © The Royal Society of Chemistry [year]

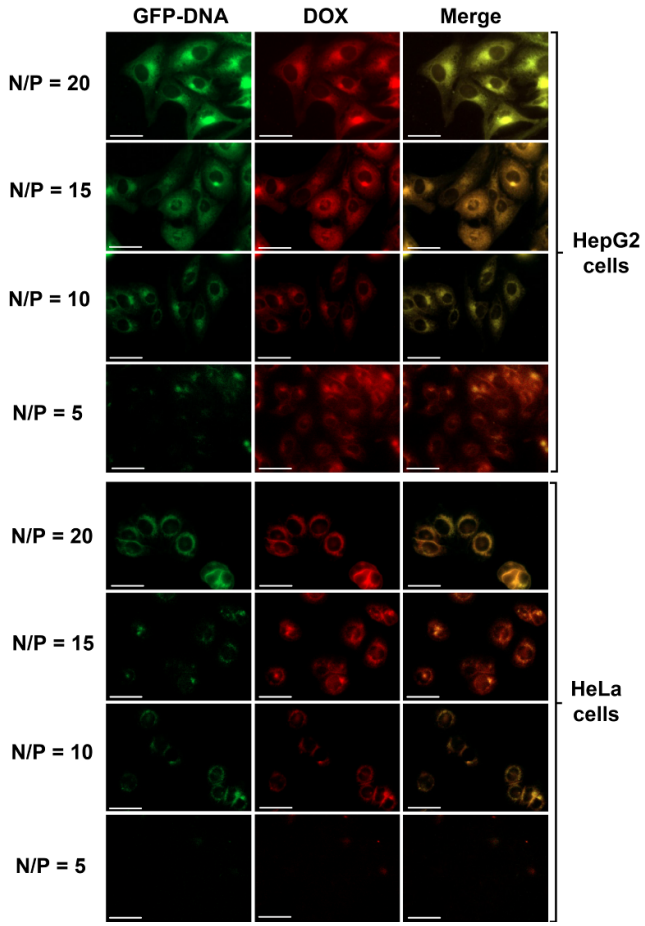

Fig. 14 Fluorescence images of HepG2 cells and HeLa cells incubated with Gal-E_{33}-*a*-C_{57}-*ss*-D_{28}/GFP-DNA/DOX polyplexes with different N/P ratios. For each panel, the images from left to right show fluorescence of GFP (green), DOX (red), and the overlays of two images. The dosage of DOX and GFP-DNA were 0.3 and 1.6 mg L^{-1}. The scale bars correspond to 50 μm in all images.

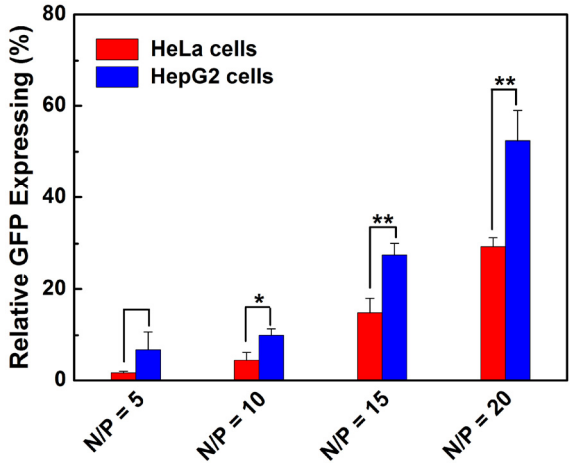

Fig. 15 Relative GFP expressing efficiency in HepG2 and HeLa cells incubated with Gal-E_{33}-*a*-C_{57}-*ss*-D_{28}/GFP-DNA/DOX polyplexes at various N/P ratios. The dose of GFP-DNA was 1.6 mg L^{-1}. Each bar represents the mean value ± SD (n = 3) (Student's t test, $*p < 0.05$, $**p < 0.01$).

Conclusions

In summary, we have reported a new kind of reduction and pH dual-responsive biodegradable micelles based on Gal-PEEP-*a*-PCL-*ss*-PDMAEMA terpolymer, which was synthesized by a combination of ROP, ATRP, CuAAC "click" reaction, and polymer reaction. The chemical structures of the terpolymers were confirmed by ^{1}H NMR, FT-IR, and GPC measurements. These triblock terpolymers could self-assemble into micelles with an average particle size less than 200 nm in aqueous solution. It should be noted that these terpolymers possess relatively low cytotoxicity, decent drug loading levels, reduction and pH dual-sensitivity, fast and maximum drug release inside cancer cells. Meanwhile, MTT assay and live cell imaging system showed that these DOX-loaded micelles prefer to internalize into HepG2 cells compared with HeLa cells through the receptor-mediated endocytosis, and DOX was rapidly released due to the reducing and acidic environment in tumor cells. More importantly, the study by a live cell imaging system further demonstrated that these terpolymer micelles could more efficiently deliver DOX and GFP-DNA into HepG2 cells than HeLa cells. This research provides a promising platform with targeted and reduction and pH dual-responsive properties aiming for simultaneous delivery of hydrophobic drugs and nucleic acids.

Acknowledgements

We gratefully acknowledge financial support from the National Natural Science Foundation of China (21374066, 21304061, 21074078), Natural Science Foundation of Jiangsu Province for Rolling Support Project (BK2011045), China Postdoctoral Science Foundation (2013M531396), Natural Science Foundation of Jiangsu Higher Education Institutions (13KJB150034), a Project Funded by the Priority Academic Program Development (PAPD) of Jiangsu Higher Education Institutions, Soochow-Waterloo University Joint Project for Nanotechnology from Suzhou Industrial Park, and Jiangsu Province Key Laboratory of Stem Cell Research (Soochow University). We are also grateful to Prof. Jian Liu (FUNSOM, Soochow University) for his valuable help in cell-related tests.

Notes and references

[a] *College of Chemistry, Chemical Engineering, and Materials Science, Jiangsu Key Laboratory of Advanced Functional Polymer Design and Application, Soochow University, Suzhou 215123, P. R. China. Tel:+86 512 65882047; E-mail: phni@suda.edu.cn (P. H. Ni); jlhe@suda.edu.cn (J. L. He)*

† Electronic Supplementary Information (ESI) available: [details of any supplementary information available should be included here]. See DOI: 10.1039/b000000x/

1. A. S. Hoffman, *J. Controlled Release*, 2008, **132**, 153-163.
2. X. L. Hu, Z. G. Xie, Y. B. Huang and X. B. Jing, *Acta Polym. Sin.*, 2013, **6**, 733-749.
3. J. Nicolas, S. Mura, D. Brambilla, N. Mackiewicz and P. Couvreur, *Chem. Soc. Rev.*, 2013, **42**, 1147-1235.
4. I. M. Verma and N. Somia, *Nature*, 1997, **389**, 239-242.
5. D. J. Wells, *Gene Ther.*, 2004, **11**, 1363-1369.
6. J. H. Jeong, S. W. Kim and T. G. Park, *Prog. Polym. Sci.*, 2007, **32**, 1239-1274.
7. M. Morille, C. Passirani, A. Vonarbourg, A. Clavreul and J. P. Benoit, *Biomaterials*, 2008, **29**, 3477-3496.

Polymer Chemistry Accepted Manuscript

8. C. H. Xu, M. H. Sui, J. B. Tang and Y. Q. Shen, *Chinese J. Polym. Sci.*, 2011, **29**, 274-287.
9. Y. Hao, M. Z. Zhang, J. L. He and P. H. Ni, *Langmuir*, 2012, **28**, 6448-6460.
10. N. Rapoport, *Prog. Polym. Sci.*, 2007, **32**, 962-990.
11. S. Ganta, H. Devalapally, A. Shahiwala and M. Amiji, *J. Controlled Release*, 2008, **126**, 187-204.
12. W. W. Gao, J. M. Chan and O. C. Farokhzad, *Mol. Pharmaceut.*, 2010, **7**, 1913-1920.
13. Y. Nie, M. Günther, Z. W. Gu and E. Wagner, *Biomaterials*, 2011, **32**, 858-869.
14. C. Deng, Y. J. Jiang, R. Cheng, F. H. Meng and Z. Y. Zhong, *Nano Today*, 2012, **7**, 467-480.
15. H. Wei, R. X. Zhuo and X. Z. Zhang, *Prog. Polym. Sci.*, 2013, **38**, 503-535.
16. E. S. Lee, Z. G. Gao and Y. H. Bae, *J. Controlled Release*, 2008, **132**, 164-170.
17. Y. Huang, Z. H. Tang, X. F. Zhang, H. Y. Yu, H. Sun, X. Pang and X. S. Chen, *Biomacromolecules*, 2013, **14**, 2023-2032.
18. S. E. Paramonov, E. M. Bachelder, T. T. Beaudette, S. M. Standley, C. C. Lee, J. Dashe and J. M. J. Fréchet, *Bioconjugate Chem.*, 2008, **19**, 911-919.
19. E. M. Bachelder, T.T. Beaudette, K. E. Broaders, J. Dashe and J. M. J. Fréchet, *J. Am. Chem. Soc.*, 2008, **130,** 10494-10495.
20. J. Z. Du, X. J. Du, C. Q. Mao and J. Wang, *J. Am. Chem. Soc.*, 2011, **133**, 17560-17563.
21. X. Guo , C. L. Shi , J. Wang , S. b. Di and S. b. Zhou, *Biomaterials*, 2013, **34,** 4544-4554.
22. Z. Y. Qiao, R. Zhang, F. S. Du, D. H. Liang and Z. C. Li, *J. Controlled Release*, 2011, **152**, 57-66.
23. J. Cheng, R. Ji, S. J. Gao, F. S. Du and Z. C. Li, *Biomacromolecules*, 2012, **13**, 173-179.
24. Y. Jin, L. Song, Y. Su, L. J. Zhu, Y. Pang, F. Qiu, G. S. Tong, D. Y. Yan, B. S. Zhu and X. Y. Zhu, *Biomacromolecules*, 2011, **12**, 3460-3468.
25. F. Lin, J. Y. Yu, W. Tang, J. K. Zheng, A. Defante, K. Guo, C. Wesdemiotis and M. L. Becker, *Biomacromolecules*, 2013, **14**, 3749-3758.
26. H. R. Wang, J. L. He, M. Z. Zhang, Y. F. Tao, F. Li, K. C. Tam and P. H. Ni, *J. Mater. Chem. B.*, 2013, **1**, 6596-6607.
27. G. Saito, J. A. Swanson and K. D. Lee, *Adv. Drug Delivery Rev.*, 2003, **55**, 199-215.
28. M. H. Lee, Z. G. Yang, C. W. Lim, Y. H. Lee, D. B. Sun, C. Kang and J. S. Kim, *Chem. Rev.*, 2013, **113**, 5071-5109.
29. M. Huo, J. Y. Yuan, L. Tao and Y. Wei, *Polym. Chem.*, 2014, **5**, 1519-1528.
30. Y. Y. Zhuang, Y. Su, Y. Peng, D. L. Wang, H. P. Deng, X. D. Xi, X. Y. Zhu and Y. F. Lu, *Biomacromolecules*, 2014, **15**, 1408-1418.
31. P. Kuppusamy, H. Q. Li, G. Ilangovan, A. J. Cardounel, J. L. Zweier, K. Yamada, M. C. Krishna and J. B. Mitchell, *Cancer Res.*, 2002, **62**, 307-312.
32. J. Chen, X. Z. Qiu, J. Ouyang, J. Kong, W. Zhong and M. M. Q. Xing, *Biomacromolecules*, 2011, **12**, 3601-3611.
33. R. Bahadur K. C., B. Thapa and P. S. Xu, *Mol. Pharmaceut.*, 2012, **9**, 2719-2729.
34. Y. J. Pan, Y. Y. Chen, D. R. Wang, C. Wei, J. Guo, D. R Lu, C. C. Chu and C. C. Wang, *Biomaterials*, 2012, **33**, 6570-6579.
35. W. Chen, P. Zhong, F. H. Meng, R. Cheng, C. Deng, J. Feijen and Z. Y. Zhong, *J. Controlled Release*, 2013, **169**, 171-179.
36. Y. F. Wen and J. K. Oh, *RSC Adv.*, 2014, **4**, 229-237.
37. F. Greco and M. J. Vicent, *Adv. Drug Delivery Rev.*, 2009, **61**, 1203-1213.
38. T. Lammers, V. Subrd, K. Ulbrichd, W. E. Hennink, G. Storm and F. Kiessling, *Nano Today*, 2010, **5**, 197-212.
39. Y. Yan, M. Björnmalm and F. Caruso, *ACS Nano*, 2013, **7**, 9512-9517.
40. L. G. Pedersen and M. Jäättelä, *Cancer Lett.*, 2013, **332**, 265-274.
41. A. R. Kirtane, S. M. Kalscheuer and J. Panyam, *Adv. Drug Delivery Rev.*, 2013, **65**, 1731-1747.
42. M. Khan, Z. Y. Ong, N. Wiradharma, A. B. E. Attia and Y. Y. Yang, *Adv. Healthcare Mater.*, 2012, **1**, 373-392.
43. J. Li, Y. Wang, Y. Zhu and D. Oupický, *J. Controlled Release*, 2013, **172**, 589-600.
44. Y. Wang, S. J. Gao, W. H. Ye, H. S. Yoon and Y. Y. Yang, *Nat. Mater.*, 2006, **5**, 791-796.
45. X. B. Xiong and A. Lavasanifar, *ACS Nano*, 2011, **5**, 5202-5213.
46. T. Liu, Y. F. Zhang and S.Y. Liu, *Chinese J. Polym. Sci.*, 2013, **31**, 924-937.
47. C. X. Liu, F. X. Liu, L. X. Feng, M. Li, J. Zhang and N. Zhang, *Biomaterials*, 2013, **34**, 2547-2564.
48. M. Saad, O. B. Garbuzenko and T. Minko, *Nanomedicine*, 2008, **3**, 761-776.
49. W. J. Xiao, X. Chen, L. Yang, Y. Q. Mao, Y. Q. Wei and L. J. Chen, *Int. J. Pharm.*, 2010, **393**, 119-126.
50. G. Shim, S. E. Han, Y. H. Yu, S. B. Lee, H. Y. Lee, K. Kim, I. C. Kwon, T. G. Park , Y. B. Kim, Y. S. Choi, C. W. Kim and Y. K. Oh, *J. Controlled Release*, 2011, **155**, 60-66.
51. T. L. Kaneshiro and Z. R. Lu, *Biomaterials*, 2009, **30**, 5660-5666.
52. S. H. Liu, Y. B. Guo, R. Q. Huang, J. F, Li, S. X. Huang, Y. Y. Kuang, L. Han and C. Jiang, *Biomaterials*, 2012, **33**, 4907-4916.
53. Y. Chen, H. R. Chen and J. L. Shi, *Mol. Pharmaceutics*, 2014, doi: 10.1021/mp400596v.
54. Y. C. Wang, Y. Y. Yaun, J. Z. Du, X. Z. Yang and J. Wang, *Macromol. Biosci.*, 2009, **9**, 1154-1164.
55. G. Y. Zhang, M. Z. Zhang, J. L. He and P. H. Ni, *Polym. Chem.*, 2013, **4**, 4515-4525.
56. Y. F. Tao, J. L. He, M. Z. Zhang, Y. Hao, J. Liu and P. H. Ni, *Polym. Chem.*, 2014, **5**, 3443-3452.
57. D. Peer, J. M. Karp, S. Hong, O. C. Farokhzad, R. Margalit and R. Langer, *Nat. Nanotechnol.*, 2007, **2**, 751-760.
58. K. Jain, P. Kesharwani, U. Gupta and N. K. Jain, *Biomaterials*, 2012, **33**, 4166-4186.
59. X. Liu, P. H. Ni, J. L. He and M. Z. Zhang, *Macromolecules*, 2010, **43**, 4771-4781.
60. H. Zhao, Q. J. Chen, L. Z. Hong, L. Zhao, J. F. Wang and C. Wu, *Macromol. Chem. Phys.*, 2011, **212**, 663-672.
61. H. Cabral, Y. Matsumoto, K. Mizuno, Q. Chen, M. Murakami, M. Kimura, Y. Terada, M. R. Kano, K. Miyazono, M. Uesaka, N. Nishiyama and K. Kataoka, *Nat. Nanotechnol.*, 2011, **6**, 815-823.

Polymer Chemistry Accepted Manuscript

This journal is © The Royal Society of Chemistry [year]